Electronic Supplementary Material (ESI) for New Journal of Chemistry.

Supporting Information:

Synthesis of mono/binuclear rhenium(I) tricarbonyl substituted with 4-mercaptopyridine related ligands: Spectral and theoretical evidence of thiolate/thione interconversion.

Alejandra Gómez,[a]* Geraldine Jara,[a] Erick Flores,[a] Tamara Maldonado,[a] Fernando Godoy,[a] Michelle Muñoz,[a] Andrés Vega,[b] Raul Mera,[c] Carlos P. Silva,[a] Jorge Pavez.[a]

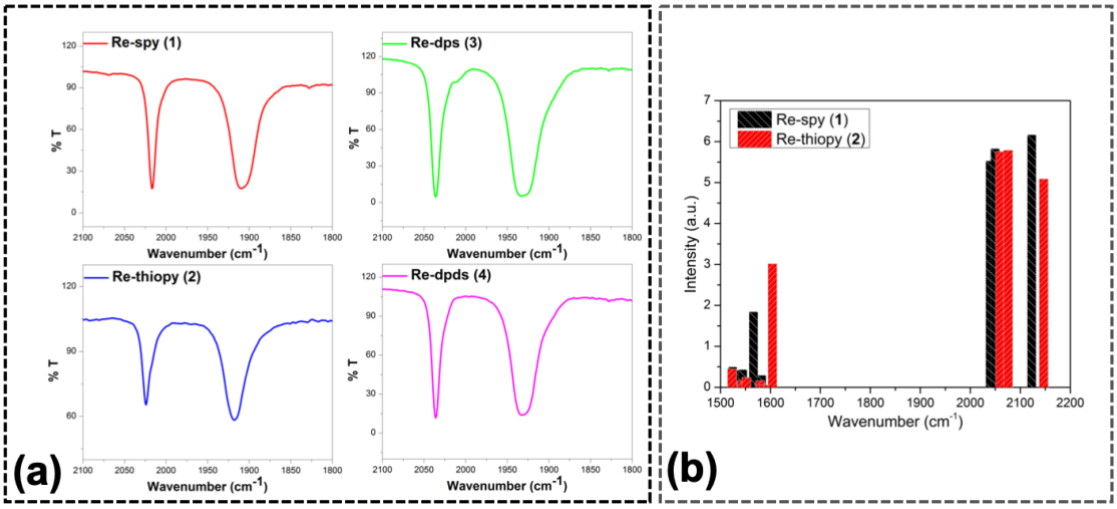

Figure S1. a) Infrared spectra measured in CH_3CN for monometallic **1**-**2** and bimetallic **3**-**4** complexes. b) IR spectra calculated for Re-spy (1) and Re-thiopy (2) in gas phase ($\nu_{M\text{-}CO}$: 2200-2000 cm^{-1}). *The frequencies for the estimation of IR absorptions were derived from Hessian matrices, obtained numerically for both systems (**1** and **2**) in gas phase at the GFN-xTB level of theory, on geometries previously optimized at the same level.*

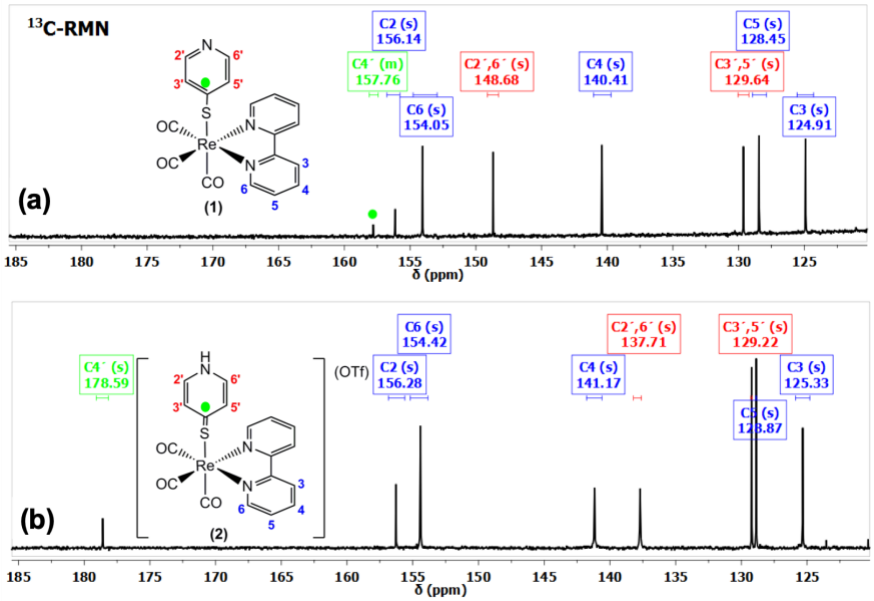

Figure S2. $^{13}C\{^{1}H\}$ NMR spectrum of (a) **1** and (b) **2** in CH_3CN-d_3 (400 MHz).

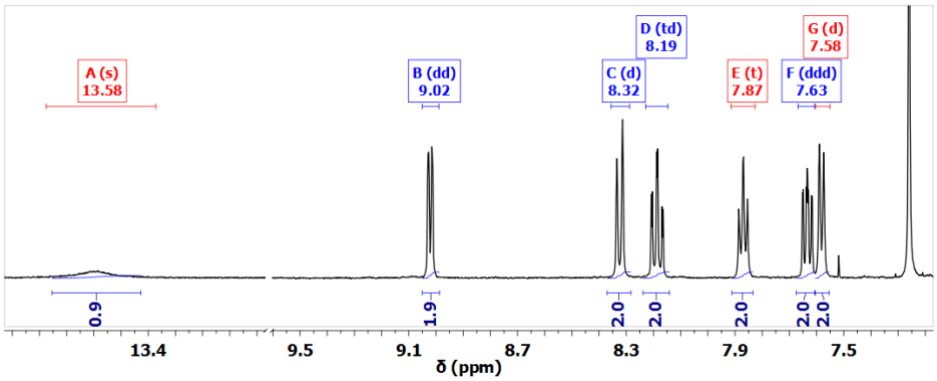

Figure S3. ^{1}H NMR spectrum of **2** in $CHCl_3$-d_1 (400 MHz).

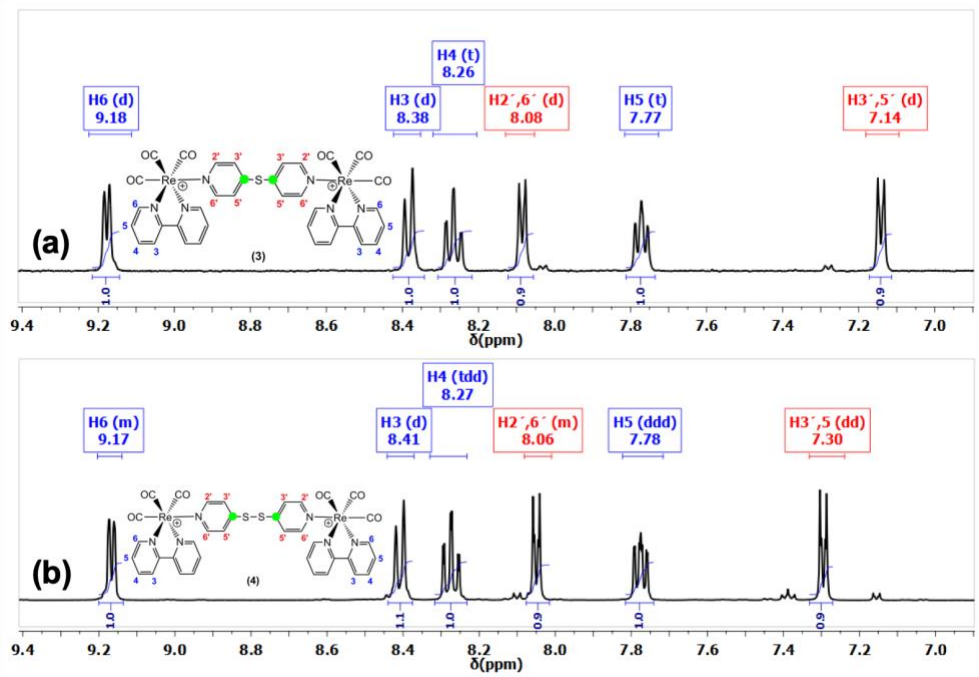

Figure S4. ^{1}H NMR spectrum of (a) **3** and (b) **4** in CH_3CN-d_3 (400 MHz).

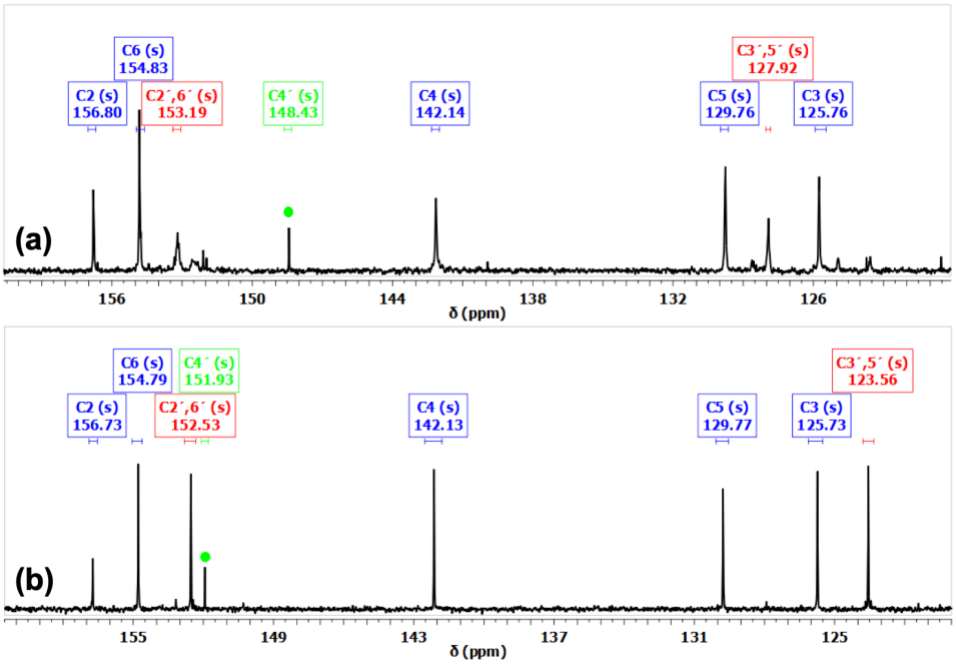

Figure S5. $^{13}C\{^{1}H\}$ NMR spectrum of (a) **3** and (b) **4** in CH_3CN-d_3 (400 MHz).

Table S1. Crystal data and structure refinement for **[$(CO)_3$(bpy)Re(μ-N,N'-$NC_5H_4SC_5H_4N$)Re(bpy)$(CO)_3$]$(CF_3SO_3)_2$ [+solvent].**

FW/uma	1339.23
Crystal System	Triclinic
Space Group	$P\bar{1}$
a (Å)	10.865(4)
b (Å)	14.038(5)
c (Å)	16.021(6)
α (°)	82.680(6)
β (°)	72.674(6)
γ (°)	89.860(7)
V (Å^3)	2312.0(14)
Z	2
d (g cm^{-3})	1.924
μ (mm^{-1})	5.46
F000	1326
θ range	2.0 to 26.0°
hkl range	$-13 \le h \le 13$
	$-17 \le k \le 17$
	$-19 \le l \le 19$
N_{tot}, N_{uniq} (R_{int}), N_{obs}	18110, 9075, 0.036, 7515
Refinement Parameters	676
GOF	1.02
R1, wR2 (obs)	0.038, 0.103
R1, wR2 (all)	
Max. and min Δρ	2.19 and -2.33

Table S2. Selected bond and interatomic distances and angles for **[$(CO)_3$(bpy)Re(μ-N,N'-$NC_5H_4SC_5H_4N$)Re(bpy)$(CO)_3$]$(CF_3SO_3)_2$ [+solvent].**

Re1—C32	1.919(7)	Re2—C36	1.921(7)
Re1—C31	1.923(7)	Re2—C35	1.925(7)
Re1—C33	1.925(7)	Re2—C34	1.921(7)
Re1—N1	2.190(5)	Re2—N4	2.166(5)
Re1—N2	2.188(5)	Re2—N3	2.183(5)
Re1—N5	2.208(5)	Re2—N6	2.205(5)
Re1···Re2	11.334(3)		
C32—Re1—C31	85.3(3)	C36—Re2—C35	86.7(3)
C32—Re1—C33	87.6(3)	C36—Re2—C34	87.6(3)
C31—Re1—C33	89.3(3)	C35—Re2—C34	89.7(3)
C32—Re1—N1	101.8(2)	C36—Re2—N4	173.6(3)
C31—Re1—N1	172.5(2)	C35—Re2—N4	99.5(3)
C33—Re1—N1	93.3(3)	C34—Re2—N4	93.9(3)
C32—Re1—N2	176.2(2)	C36—Re2—N3	98.9(3)
C31—Re1—N2	98.2(2)	C35—Re2—N3	174.1(2)
C33—Re1—N2	90.9(3)	C34—Re2—N3	92.1(2)
N1—Re1—N2	74.8(2)	N4—Re2—N3	74.8(2)
C32—Re1—N5	93.4(2)	C36—Re2—N6	93.3(2)
C31—Re1—N5	91.1(3)	C35—Re2—N6	92.6(2)
C33—Re1—N5	178.9(3)	C34—Re2—N6	177.6(2)
N1—Re1—N5	86.15(19)	N4—Re2—N6	84.95(18)
N2—Re1—N5	88.01(18)	N3—Re2—N6	85.54(18)
C23—S1—C28	103.3(3)		

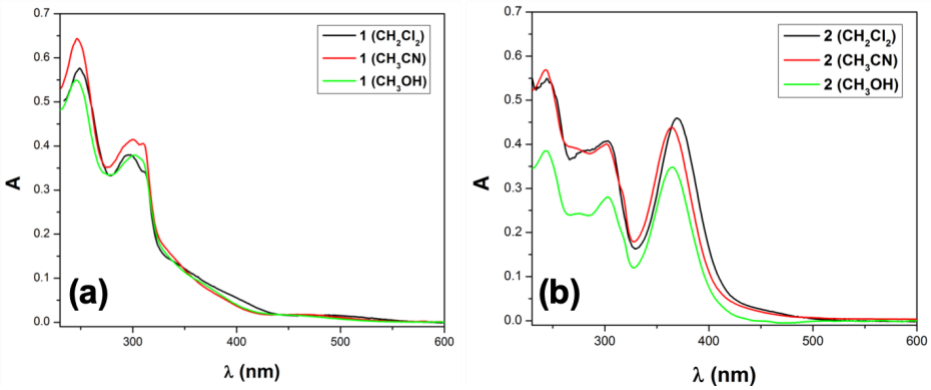

Figure S6. UV-Vis spectrum of (a) **1** and (b) **2** measured in CH_2Cl_2, CH_3CN, CH_3OH.

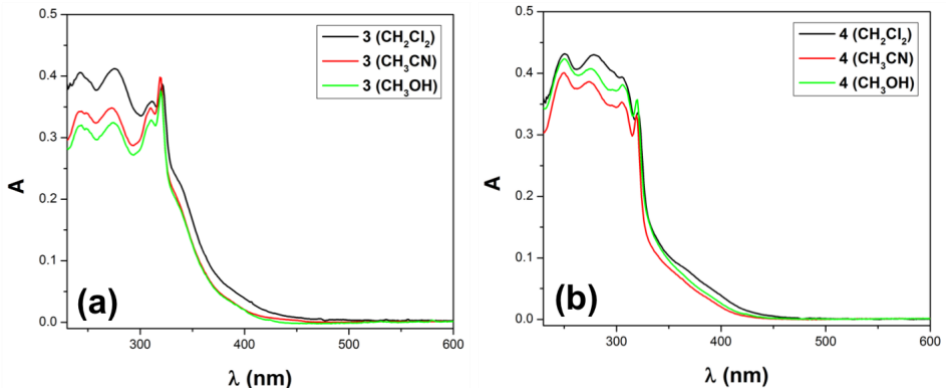

Figure S7. UV-Vis spectrum of (a) **3** and (b) **4** measured in CH_2Cl_2, CH_3CN, CH_3OH.

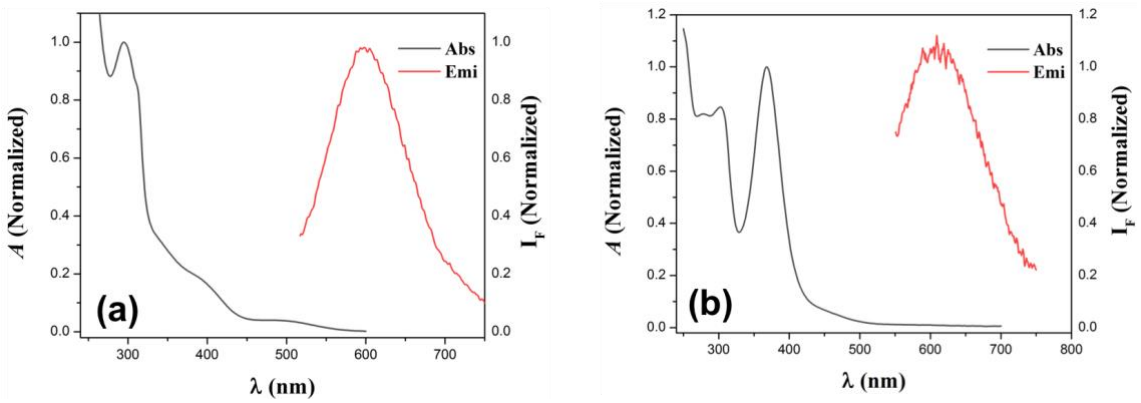

Figure S8. Electronic absorption (black trace) and emission (red trace) of (a) **1** and (b) **2** (λ_{exc}: 435 nm) measured in aerated CH_2Cl_2 at room temperature.

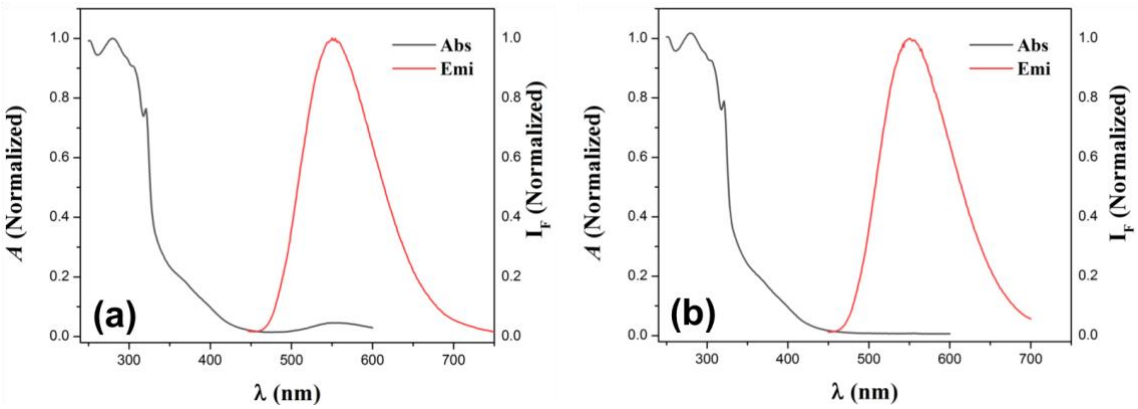

Figure S9. Electronic absorption (black trace) and emission (red trace) of (a) **3** and (b) **4** (λ_{exc}: 425 nm) measured in aerated CH_2Cl_2 at room temperature.

Quantum yields (Φ_F) were determined using the follow expression:

$$\Phi_x = \Phi_{st}\left(\frac{Grad_x}{Grad_{st}}\right)\left(\frac{\eta_x^2}{\eta_{st}^2}\right)$$

Where:

Φ_x: Quantum yield of the sample.

Φ_{st}: Quantum yield of the standard.

η_x: Refraction index of the solvent used for measuring the sample.

η_{st}: Refraction index of the solvent used for measuring the standard.

$Grad_x$; $Grad_{st}$: Slopes obtained in of the plot of integrated fluorescence intensity versus the absorbance at the excitation wavelength of the standard and the sample, respectively.

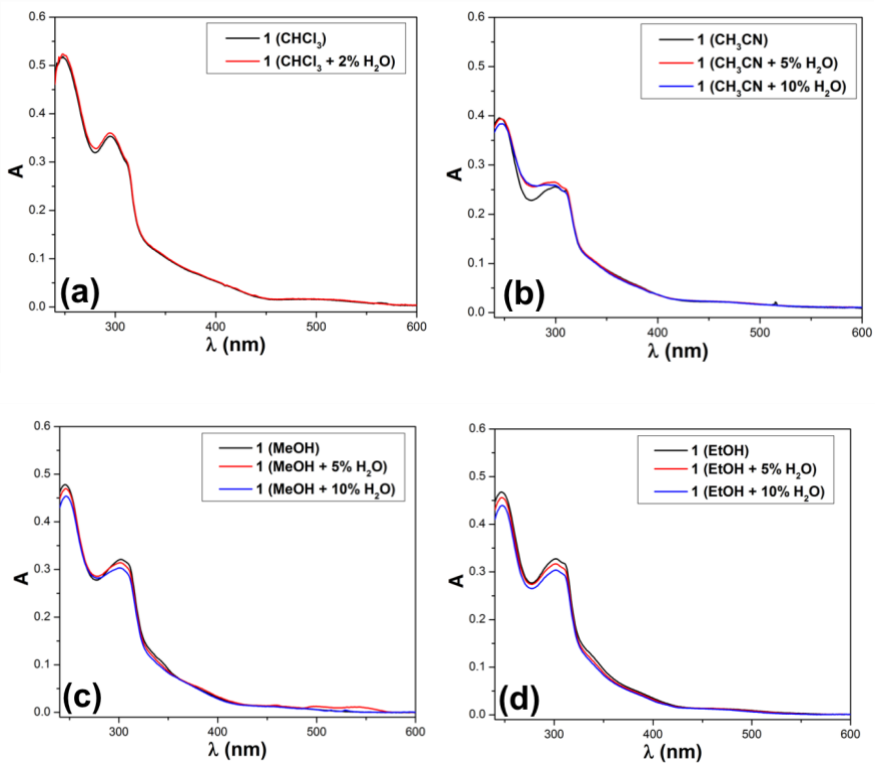

Figure S10. UV-Vis spectrum of **1** measured in different solvents as $CHCl_3$, CH_3CN, CH_3OH, EtOH and respective addition of water.

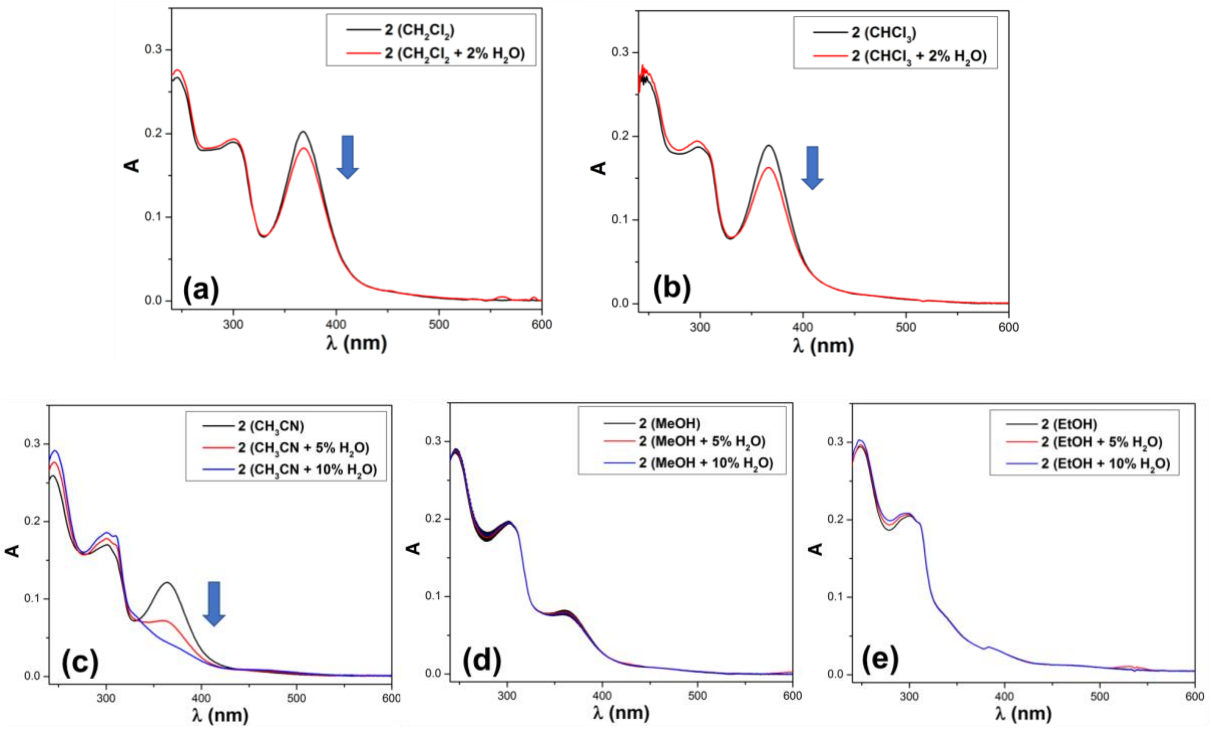

Figure S11. UV-Vis spectrum of **2** measured in different solvents as CH_2Cl_2, $CHCl_3$, CH_3CN, CH_3OH, EtOH and respective addition of water.

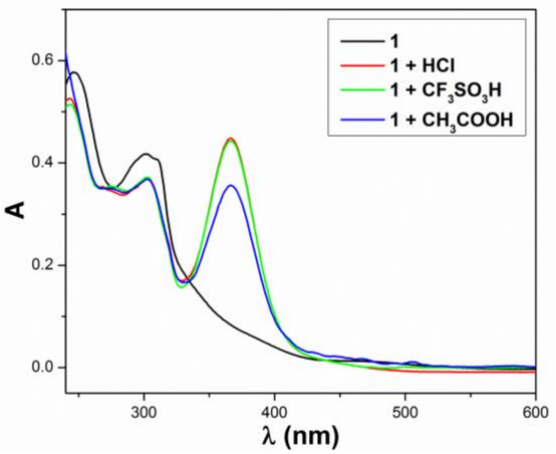

Figure S12. UV-Vis spectrum of **1** measured in EtOH after the addition of acids such as HCl, CH_3COOH, HSO_3CF_3.

Theoretical calculations. **Solvated structures.** The optimized structure for **1** was placed at the center of a sphere containing 130 methanol molecules by using Packmol [1]. One water molecule was placed close to the solute to mimic the experimental conditions. A 6 ps full quantum-chemical, with the GFN2-xTB semiempirical method[2], Langevin molecular dynamics simulation in spherical-boundary conditions at 298 K, was performed on the system, after a 300-steps equilibration. The system was then subject to 2610 optimization steps at the same level. Both the MD and the optimization calculations employed a generalized Born-based continuum model solvent with the methanol parameters included in the program. All semiempirical calculations were performed with the xtb program v6.2 (https://github.com/grimme-lab/xtb), while the molecular dynamic and optimization steps were guided by the pDynamo libraries v1.9.0[3]. The solute and two solvent molecules, judged important for the studied effect, were separated from the final structure and employed for UV-vis spectra calculation without further optimization, in order to avoid disrupting the solvated geometry.

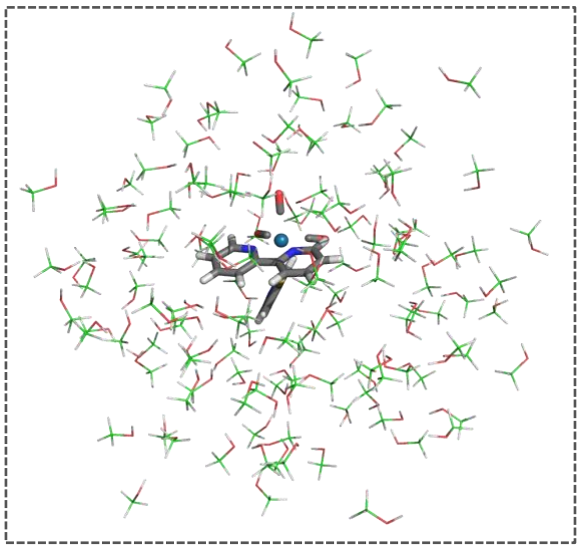

Figure S13. Visualization of the full system: Re-spy with a sphere of 130 methanol molecules, and one water molecule.

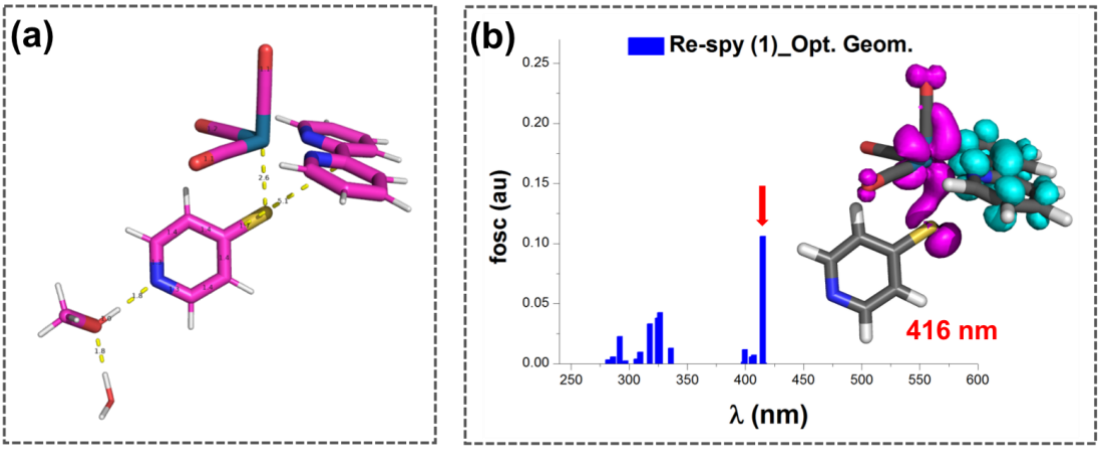

Figure S14. Re-spy (**1**)..MeOH..H_2O **a)** Structure of solvated geometry. **b)** Simulated electronic spectra for optimized geometry after and electronic density difference analysis surfaces.

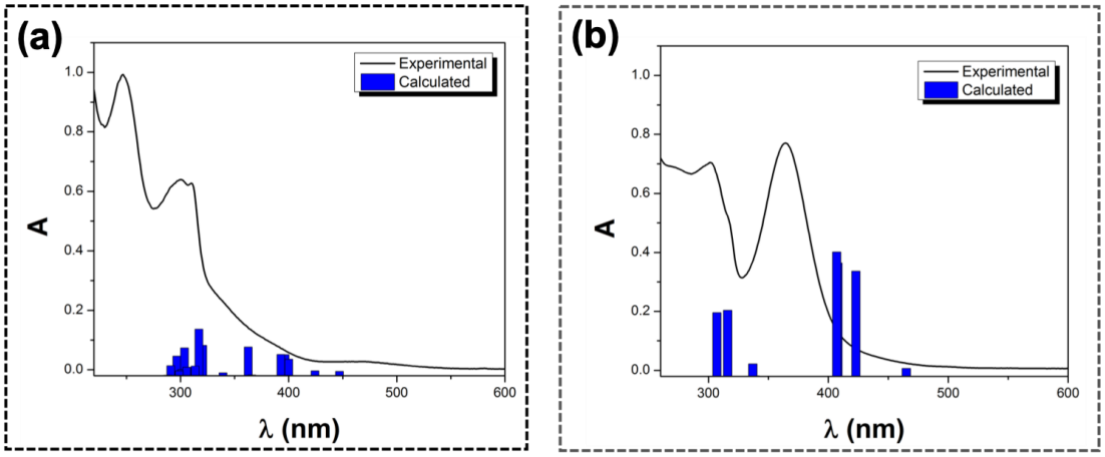

Figure S15. ADC(2) ab-initio level calculations for **a)** Re-spy (**1**) and **b)** Re-thiopy (**2**).

Table S3. Summary of Electrochemical Data for the redox behavior of rhenium(I) tricarbonyl complexes

Complex	$E_{1/2}$ (I/I`) /V	E_{pc} (I) /V	E_{pa} (I´) /V	E_{pc} (II) /V	E_{pa} (II´) /V	E_{pc} (III) /V	E_{pa} (III´) /V
Re-spy (**1**)	-1.681	-1.727	-1.635	-2.119	-1.495	--	--
Re-thiopy (**2**)	-1.689	-1.742	-1.636	-2.089	-1.516	--	--
Re-dps (**3**)	-1.533	-1.581	-1.485	-2.049	-1.636	-1.032	-0.060
Re-dpds (**4**)	-1.509	-1.557	-1.461	-2.060	-1.627	-1.152	0.094
(bpy)Re(CO)$_3$Cl	-1.670	-1.710	-1.620	-2.110	-1.540	--	--

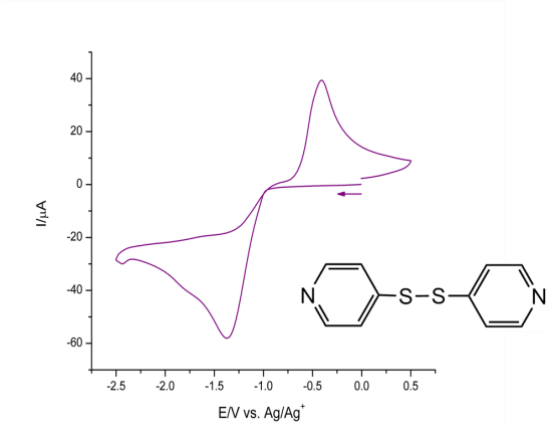

Figure S16. Cyclic voltammogram of 4,4´-dipyridyldisulfide (dpds); scan rate: 0.5 V/s. (dpds) in dry CH_3CN.

References

[1] L. Martínez, R. Andrade, E. G. Birgin, J. M. Martínez, J. *Comput. Chem.* 2009, **30**, 2157–2164.
[2] C. Bannwarth, S. Ehlert, S. Grimme, S., *J. Chem. Theory Comput.* 2019, **15**, 1652–1671.
[3] M. J. Field, *J. Chem. Theory Comput.* 2008, **4**, 1151–1161.